Assessing the Impact of Wind Variability on Power System Small-Signal Reachability

Yu Christine Chen and Alejandro D. Domínguez-García
Department of Electrical and Computer Engineering
University of Illinois at Urbana-Champaign
Urbana, IL, USA
Email: {chen267, aledan}@ILLINOIS.EDU

Abstract—We propose a method to assess the impact on power system dynamic performance of operational uncertainty caused by variability in the system supply side. Operational uncertainty is not new to power systems, e.g., demand variability. However, with the increased penetration of renewable-based generation, operational uncertainty will extend to a significant portion of the supply side, which may have an impact on system dynamic performance, e.g., frequency or voltage deviations beyond prescribed operational requirements. To address the problem, we propose the use of reachability analysis techniques, which will provide bounds on worst-case deviations of system variables that must remain within certain bounds. The method is illustrated with several examples.

I. INTRODUCTION

The push toward energy independence and a cleaner environment entails increased penetration of renewable resources in the power grid. It has long been acknowledged that the integration of these resources presents major challenges in operations and planning of today's power systems [1], [2], [3]. For example, the highly variable nature of wind speeds not only makes the wind resource highly intermittent but presents major difficulties in accurate forecasting [4]. Therefore, the integration of wind presents an additional source of uncertainty in the management of these non-dispatchable units. This uncertainty affects operations planning—power system operators, faced with the lack of control of these units, must compensate by bringing additional insurance for their system through the increase in the level of reserves [5]. Deep levels of wind penetration in the system also have an impact on system dynamic performance, i.e., small-signal and transient stability [6]. In this regard, it has been acknowledged that, as the presence of wind in the power grid increases, new tools are necessary to assess the impact of wind on the security of supply and load balancing in near real time [7].

This paper focuses on this last problem—the impact of wind penetration on system dynamic performance. In particular, *we address how system variables may deviate from prescribed values imposed by operational requirements due to the uncontrolled variability of the wind resource*. We provide an analytically tractable method, amenable for computer implementation, to assess whether certain variables of interest, such as system frequency and bus voltages, remain within acceptable ranges while the system is subjected to uncontrolled disturbances caused by the variability of the wind resource. We envision this method to be used in operations, as it provides operators with a metric of how close the time-evolved system may be from violating certain performance requirements given the amount of available wind-based generation and its expected variability on a particular time window.

We assume that power system dynamics are described by the classical nonlinear differential-algebraic equation (DAE) representation [8], where the effect of the wind resource is modeled as an uncontrolled (and not perfectly known due to forecast error) disturbance to the system dynamics. In this setup, the problem can be addressed by computing the reach set or attainability domain [9], i.e., the set that bounds all possible system trajectories that arise from all possible wind power scenario realizations. Computing the exact shape of the reach set can be very difficult, or even impossible, especially for nonlinear DAEs. Thus, instead of computing the reach set for the nonlinear DAE description, we assume that the disturbance introduced by wind variability is small enough to justify the use of a small-signal model. Then, the DAE model is linearized around some nominal trajectory, which is determined by the wind forecast. For the period of study (ranging from minutes to hours), the wind forecast error provides bounds on the variability of wind-based generation injected in the system. These

bounds are used together with the linearized model to compute the reach set, which provides bounds on worst-case deviations of system variables of interests, e.g., frequency and voltage at certain buses for all possible wind power scenario realizations. If the reach set is within the region of the state-space defined by system operational requirements, e.g., maximum frequency deviation and maximum voltage excursions on certain buses, then we can conclude that wind variability does not have a significant impact on system dynamic performance.

The reachability problem in power systems subject to uncertainties has been addressed before in the context of power flow analysis, without consideration to dynamic issues (e.g., see [10], [11], [12] and the references therein). Reachability analysis has also been used in power systems transient stability analysis for computing the domain of attraction of an equilibrium point [13].

The remainder of this paper is structured as follows. In Section II, the system model is presented, reachability concepts are introduced and a method to solve the reachability problem is provided. Also, in this section, we illustrate the application of reachability analysis to a single-machine infinite-bus (SMIB) system, where we quantify the impact on the machine dynamic variables of deviations on the infinite bus voltage magnitude. Section III extends the ideas of Section II and develops a method to study the impact of variations in wind-based power generation injected in a power system. Section IV illustrates the application of this method to a three-bus system with one conventional generator, one negative load representing the aggregate power generated from wind injected in the system, and one additional (positive) load representing the system demand. Concluding remarks are presented in Section V.

II. PRELIMINARIES

Electric power systems are usually represented by a nonlinear DAE of the form [8]

$$
\begin{aligned}
\dot{x} &= g(x, y, u), \\
0 &= h(x, y, w), \\
x(0) &= x_0, \ y(0) = y_0,
\end{aligned} \tag{1}
$$

where $x \in \mathbb{R}^n$ includes machine dynamic states such as angles, velocities, and the synchronous machine torque; the input $u \in \mathbb{R}^m$ includes set points, such as voltage regulator reference and steam valve position; and $w \in \mathbb{R}^l$ includes uncontrolled disturbances such as load demand changes or wind speed variability as discussed in Section III.

In the context of this work, we assume that system (1) is operating with some nominal $u(t) = u^*$ and the disturbance $w(t)$ can take values around some nominal (possibly time-varying) w^*. Furthermore, we assume for $t \in [0, T]$, the maximum variations of $w(t)$ around w^* are bounded. Thus the disturbance $w(t)$ is assumed to belong to a (possibly time-varying) set $\mathcal{W}$. This disturbance model could represent worst-case forecast error for the entries of w, which may include load demand and wind speed.

A. Nonlinear Ordinary Differential Equation Model

Let (x^*, y^*) be the system trajectory that results from the nominal $u(t) = u^*$ and $w(t) = w^*$ and with initial conditions $x(0) = x_0$ and $y(0) = y_0$. We also assume that $h(\cdot, \cdot, \cdot)$ is continuously differentiable at each point of an open set $\mathcal{S}$ and $h(x^*, y^*, w^*) = 0$. If the Jacobian matrix $[\partial h / \partial y]_{(x^*, y^*, w^*)}$ is non-singular, then there exists function ϕ such that $y = \phi(x, w)$ locally around (x^*, y^*, w^*). Thus, around the nominal system trajectory (x^*, y^*), system (1) can be rewritten as

$$
\dot{x} = g(x, \phi(x, w), u^*). \tag{2}
$$

In other words, it is possible to obtain an ordinary differential equation (ODE) from system (1) that is valid locally around some nominal trajectory. This is a direct result of the implicit function theorem and has been stated before in the context of trajectory sensitivity analysis of power systems [14], [15].

Thus, in the context of this work, and without loss of generality, we describe the dynamic behavior of electric power systems by a nonlinear ODE of the form

$$
\begin{aligned}
\dot{x} &= f(x, u^*, w), \\
x(0) &= x^*(0), \\
w(t) &\in \mathcal{W}, \ w(0) = w^*(0).
\end{aligned} \tag{3}
$$

If system (3) is forward complete, then the solution $x(t)$ exists for for $t \in [0, T]$ and it is contained in some set $\mathcal{R}$, which is called the reach set or attainability domain [16].

Although the shape of $\mathcal{W}$ is arbitrary, it can always be bounded by an ellipsoid Ω_w defined as

$$
\Omega_w = \{w : (w - w^*)' Q^{-1} (w - w^*) \leq 1\}, \tag{4}
$$

such that $\mathcal{W} \subseteq \Omega_w$. As it turns out, the set $\mathcal{W}$ is usually a symmetrical polytope, i.e., each entry in w is assumed to lie within some interval. A symmetrical polytope can always be approximated to a high degree of precision by the intersection of a family of ellipsoids, each of which is

tight to the polytope in a specific direction. When several ellipsoids are used to bound the disturbance set $\mathcal{W}$, the reach set $\mathcal{R}$ can be computed for each of the ellipsoids bounding $\mathcal{W}$, and then the intersection of the resulting reach sets (for each bounding ellipsoid) yields a high-fidelity approximation of the exact reach set $\mathcal{R}$. With this in mind, and to simplify subsequent developments, we will assume that the disturbance set is indeed described by the ellipsoid Ω_w, and thus the system dynamics is now described by

$$
\begin{aligned}
\dot{x} &= f(x, u^*, w), \\
x(0) &= x^*(0), \\
w(t) \in \Omega_w &= \{w : (w - w^*)' Q^{-1} (w - w^*) \le 1\}.
\end{aligned} \quad (5)
$$

Even if the disturbance set is defined by an ellipsoid as in (5), the computation of the exact reach set $\mathcal{R}$ is a difficult task. This computation often relies on time-domain simulations for different realizations of the input. There is also a connection between reachability analysis and input-to-state-stability (ISS) [17], with some recent work on the application of ISS notions to the computation of reach sets in power system subject to uncertain inputs [18].

B. Linearized Model

We apply notions from optimal control to describe the perturbations in $x(t)$ that result from perturbing w around w^* [19]. If the variations of the disturbance $w(t)$ around w^* in (5) are sufficiently small, then we can approximate $\mathcal{R}$ by the reach set of the system that results from linearizing (5).

Let $x(t) = x^* + \Delta x$ and $w(t) = w^* + \Delta w$, where $\Delta w \in \Delta \mathcal{W}$, and $\Delta \mathcal{W}$ is such that $\mathcal{W} = w^* \oplus \Delta \mathcal{W}$. While the shape of $\Delta \mathcal{W}$ is arbitrary, it can always be bounded by an ellipsoid $\Omega_{\Delta w}$:

$$
\Delta w \in \Omega_{\Delta w} = \{\Delta w : \Delta w' Q(t)^{-1} \Delta w \le 1\}. \quad (6)
$$

Then, small variations in the system trajectories, denoted by Δx, originating from small variation of the system input, denoted by Δw, can be approximately obtained from

$$
\begin{aligned}
\tfrac{d\Delta x}{dt} &= A\Delta x + B\Delta w, \\
\Delta x(0) &= 0, \\
\Delta w \in \Omega_{\Delta w} &= \{\Delta w : \Delta w' Q^{-1} \Delta w \le 1\},
\end{aligned} \quad (7)
$$

where $A = \frac{\partial f(x,u,w)}{\partial x}\big|_{x^*,u^*,w^*}$, $B = \frac{\partial f(x,u,w)}{\partial w}\big|_{x^*,u^*,w^*}$.

C. Linearized model Reach Set Computation

The reach set of (7), denoted by $\Delta \mathcal{R}$, contains (for all $t \ge 0$) all possible trajectories of the Δx approximations, and can be obtained as the intersection of a family of ellipsoids:

$$
\Delta \mathcal{R} = \bigcap_\eta \mathcal{X}_\eta, \ \forall \eta \in \mathbb{R}^n \text{ such that } \eta' \eta = 1, \quad (8)
$$

with $\mathcal{X}_\eta = \{x : x' \Psi_\eta^{-1} x \le 1\}$, where for each η, Ψ_η is obtained by solving

$$
\begin{aligned}
\tfrac{d\Psi_\eta}{dt} &= A\Psi_\eta + \Psi_\eta A' + \beta_\eta \Psi_\eta + \tfrac{1}{\beta_\eta} BQB', \\
\beta_\eta &= \sqrt{\tfrac{\eta' BQB' \eta}{\eta' \Psi_\eta \eta}}.
\end{aligned} \quad (9)
$$

The reader is referred to [20] for a derivation of (9).

Each of the ellipsoids in (8) is tangent to the reach set $\Delta \mathcal{R}$ at exactly two points. Even if $\Delta \mathcal{R}$ is the exact reach set of the system in (7), since this system is an small-signal approximation, $\Delta \mathcal{R}$ is just an approximation of the reach set $\mathcal{R}$ for the system (3). Thus, in most practical cases, sufficiently accurate results are obtained with the computation of a few ellipsoids of the family in (8).

D. Dynamic Performance Requirements

The computation of the reach set allows us to determine whether or not the system violates certain performance requirements that impose bounds on the maximum excursions of certain system variables. For example in the Western Electricity Coordinating Council (WECC) system, the acceptable frequency range requirement is between 59.4 Hz and 60.6 Hz [21]. Constraints in the form of interval ranges on other variables of interest include voltage at certain buses and machine speed fluctuations.

Then, without loss of generality, dynamic performance requirements will constrain the excursion of the state-vector x around x_0 to some region of the state-space Φ defined by the symmetric polytope

$$
\Phi = \{x : |\pi_i'\, (x - x_0)| \le 1 \ \forall i = 1, 2, \ldots, p\}, \quad (10)
$$

where $\pi_i \in \mathbb{R}^n$ is a column vector.

Then, checking that the system meets all the dynamics performance requirements for any $w(t) \in \Omega_w$, with $t \in [0, T]$, is equivalent to checking that $\Delta \mathcal{R} \subseteq \Phi$.

E. Single-Machine Infinite-Bus System Example

We illustrate the application of the concepts introduced above to the single-machine infinite-bus (SMIB) system of Fig. 1, where the infinite bus voltage fluctuates
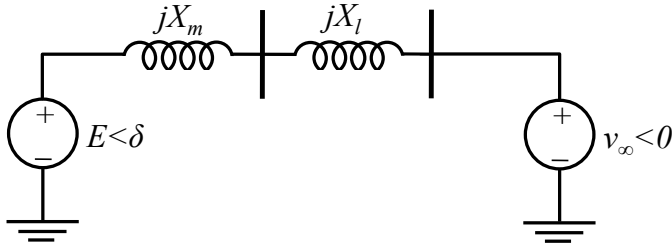
Fig. 1. Single-machine infinite bus system.

over time. However, the time structure of this fluctuation is not known except for upper and lower bounds.

Let δ be the angular position of the rotor in electrical radians, and ω be the angular velocity of the rotor in electrical rad/s. Then, the system can be described by the following state-space representation:

$$\frac{d}{dt}\begin{bmatrix} \delta \\ \omega \end{bmatrix} = \begin{bmatrix} 0 & 1 \\ 0 & -\frac{D}{M} \end{bmatrix}\begin{bmatrix} \delta \\ \omega \end{bmatrix} + \begin{bmatrix} -1 \\ \frac{D}{M} \end{bmatrix}\omega_s$$
$$+ \begin{bmatrix} 0 \\ -\frac{E}{M(X_m+X_l)}\sin\delta \end{bmatrix}v_\infty + \begin{bmatrix} 0 \\ \frac{1}{M} \end{bmatrix}T_m,$$
$$v_\infty \in \Omega_{v_\infty} = \{v_\infty : |v_\infty - v_m| \le kv_m\}, \quad (11)$$

with $k > 0$, $v_m > 0$, and where D, M, E, X_m, X_l, ω_s, and T_m are constant parameters [8].

For $v_\infty = v_m$, the (stable) equilibrium point of the system (11) is given by

$$\omega_0 = \omega_s,$$
$$\delta_0 = \sin^{-1}\left(\frac{T_m}{\frac{Ev_m}{X_m+X_l}}\right) \in \left[0, \frac{\pi}{2}\right]. \quad (12)$$

Following the notation of (7), small variations of state

variables around the equilibrium point (12) are given by

$$\frac{d}{dt}\begin{bmatrix} \Delta\delta \\ \Delta\omega \end{bmatrix} = \begin{bmatrix} 0 & 1 \\ \frac{Ev_m}{M(X_m+X_l)}\cos\delta_0 & -\frac{D}{M} \end{bmatrix}\begin{bmatrix} \Delta\delta \\ \Delta\omega \end{bmatrix}$$
$$+ \begin{bmatrix} 0 \\ -\frac{T_m}{Mv_m} \end{bmatrix}\Delta v_\infty,$$
$$\Delta v_\infty \in \Omega_{\Delta v_\infty} = \{\Delta v_\infty : |\Delta v_\infty| \le kv_m\}. \quad (13)$$

Reachability analysis of the system (13) was conducted using the parameter values of Table I, where, unless specified, all the values are given in per unit. A few ellipsoids of the ellipsoidal family, the intersection of which yields the linearized system reach set, are represented in Fig. 2(a) with dashed traces. In the same figure, the reach set is represented with a solid trace. In Fig. 2(b), the linearized model reach set (centered around the equilibrium point) is depicted with a dashed line. In the same figure, a system trajectory obtained from (11) is plotted, where v_∞ jumps from 0.9 (minimum value) to 1.1 (to its maximum value) whenever the norm of the state vector starts decreasing. In terms of excursions of the state variables, this is the worst possible input. It can be seen that the linearized small-signal reach set fully contains this trajectory. It also can be seen, that the linearized system reach set is contained within the region defined by the two horizontal solid traces, which correspond to the acceptable frequency range of the WECC system.
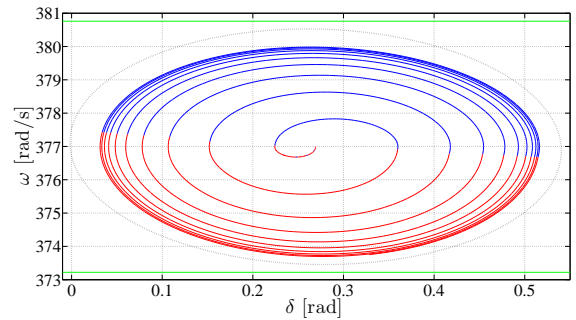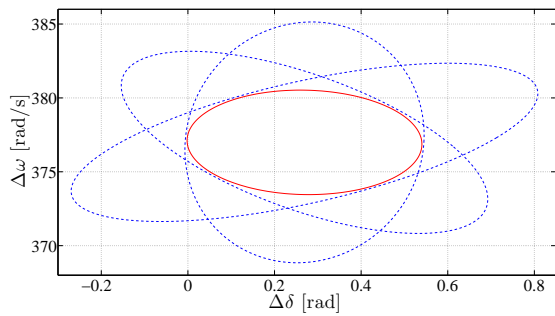
(a) Tight ellipsoidal bounds of the linearized model reach set and reach set obtained as the intersection of the tight ellipsoidal family.

(b) Large-signal worse-case trajectory and linearized model reachability set.

Fig. 2. Single-machine infinite bus system reachability analysis results.

III. APPLICATION OF REACHABILITY ANALYSIS TO ASSESSING THE IMPACT OF WIND VARIABILITY

In this section, the reachability notions presented in the previous section are used to assess the impact of the variability of the wind resource on the dynamics of certain dynamic variables of interest.

A. Wind Power Injection Model

We assume that the power injected in the system by a wind farm can be modeled as a negative load. Thus, in any given system bus, a power injection can represent an aggregated model of a single wind farm connected directly to that node, or it could represent an aggregated model of several wind farms within the same geographical area.

This power injection is dependent on the wind speed. Thus, for a time horizon $0 \leq t \leq T$, if bounds on the wind speed forecast error are known, it is possible to bound the power injected at a node by a single farm or a collection of farms. Assume the system has n nodes. Let $P_{w,i}(t)$ be the power injected in node i generated from wind at time $t \in [0, T]$. Let $P_m^i(t) > 0$ be the forecast wind power at time $t \in [0, T]$. Then, $P_w^i(t)$ can be described by

$$
\begin{aligned}
P_w^i(t) \in \Omega_{P_w^i}(t) = \\
\{|P_w^i(t) - P_m^i(t)| \leq k_w^i(t)P_m^i(t)\},
\end{aligned}
\tag{14}
$$

with $i = 1, 2, \ldots, n$, and where $k_w^i(t) \geq 0$ depends on the wind forecast error at time $t \in [0, T]$.

B. Linearized Power System Model

Let $\Delta P_w^i(t)$ the variation of wind power injection around the forecast value $P_m^i(t)$. Then

$$
\begin{aligned}
\Delta P_w^i(t) \in \Omega_{\Delta P_w^i}(t) = \\
\{|\Delta P_w^i(t)| \leq k_w^i(t)P_m^i(t)\}.
\end{aligned}
\tag{15}
$$

Let $\Delta P_w(t) = [\Delta P_w^1(t), \Delta P_w^2(t), \ldots, \Delta P_w^n(t)]$ be the vector of wind power injections. Then, $\Delta P_w(t) \in \Delta \Omega_{\Delta P_w}(t)$, where

$$
\begin{aligned}
\Delta \Omega_{P_w}(t) = \\
\Delta \Omega_{P_w^1}(t) \times \Delta \Omega_{P_w^2}(t) \times \cdots \times \Delta \Omega_{P_w^n}(t),
\end{aligned}
\tag{16}
$$

is the set of wind power injections. Then, assuming the wind power injection model of (15) and (16). Then, the linearized power system model can be described by

$$
\begin{aligned}
\frac{d\Delta x}{dt} &= A\Delta x + B\Delta P_w, \\
\Delta x(0) &= 0, \\
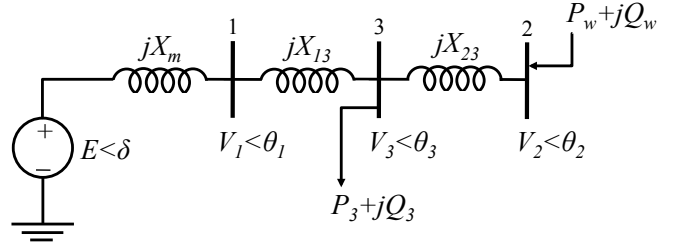\Delta P_w(t) &\in \Omega_{\Delta P_w}(t).
\end{aligned}
\tag{17}
$$

Fig. 3.   Three-bus system with wind.

C. Reach Set Computation

By definition, $\Delta \Omega_{\Delta P_w}(t)$ is an n-dimensional symmetrical polytope centered around zero. Thus, the ellipsoidal techniques presented in Section II-C cannot be directly used to compute the reach set of (17). As discussed before, we can circumvent this problem by bounding the polytope $\Delta \Omega_{\Delta P_w}(t)$ by a single ellipsoid that is the minimum volume ellipsoid containing the set of all possible realizations of the input and ellipsoidal techniques can be used to compute an upper-bound on the reach set of (17). If a more accurate solution is needed, polytope $\Delta \Omega_{\Delta P_w}(t)$ can be bounded by a family of ellipsoids, each of which is tight to $\Delta \Omega_{\Delta P_w}(t)$ in a specific direction.

IV. THREE-BUS SYSTEM WITH CONVENTIONAL AND WIND-BASED GENERATION

The ideas described above are applied to the three-bus system with wind-based power generation as depicted in Fig. 3. In this system, a synchronous machine is connected to bus 1. As in the SMIB example, a classical model is used to describe the machine dynamics, but this model has been augmented with one more equation to describe the governor model, so the mechanical torque T_m becomes an additional state variable, and the valve position P_s becomes an external reference. Wind power is injected at bus 2 and there is a load in bus 3.

The synchronous machine model connected to bus 1 is given by

$$
\frac{d}{dt}
\begin{bmatrix}
\delta \\
\omega \\
T_m
\end{bmatrix}
=
\begin{bmatrix}
0 & 1 & 0 \\
0 & -\frac{D}{M} & \frac{1}{M} \\
0 & -\frac{1}{T_{SV}R_D\omega_s} & -\frac{1}{T_{SV}}
\end{bmatrix}
\begin{bmatrix}
\delta \\
\omega \\
T_m
\end{bmatrix}
$$
$$
+
\begin{bmatrix}
0 \\
-\frac{EV_1}{MX_m}\sin(\delta - \theta_1) \\
0
\end{bmatrix}
+
$$
$$
+
\begin{bmatrix}
-1 \\
\frac{D}{M} \\
\frac{1}{\omega_s T_{SV}R_D}
\end{bmatrix}
\omega_s
+
\begin{bmatrix}
0 \\
0 \\
\frac{1}{T_{SV}}
\end{bmatrix}
P_c.
\tag{19}
$$

The wind-based power generation injection model at bus 2 is given by

$$P_w(t) \in \Omega_{P_w} = \{P_w : |P_w - P_m| \leq k_w P_m\},$$
$$Q_w(t) = Q_w, \quad (20)$$

where P_m, k_w, and Q_w are constants. The power balance equations for bus 1 are given by

$$Y_m E V_1 \sin(\delta - \theta_1) = Y_{13} V_1 V_3 \sin(\theta_1 - \theta_3), \quad (21)$$
$$Y_m E V_1 \cos(\delta - \theta_1) - Y_m V_1^2 =$$
$$-Y_{13} V_1 V_3 \cos(\theta_1 - \theta_3) + (Y_{13} + Y_m) V_1^2. \quad (22)$$

The power balance equations for bus 2 are given by

$$P_w = Y_{23} V_2 V_3 \sin(\theta_2 - \theta_3), \quad (23)$$
$$Q_w = -Y_{23} V_2 V_3 \cos(\theta_2 - \theta_3) + Y_{23} V_2^2. \quad (24)$$

The power balance equations for bus 3 are given by

$$-P_3 = Y_{13} V_1 V_3 \sin(\theta_3 - \theta_1)$$
$$+Y_{23} V_2 V_3 \sin(\theta_3 - \theta_2), \quad (25)$$
$$-Q_3 = -Y_{13} V_1 V_3 \cos(\theta_3 - \theta_1)$$
$$-Y_{23} V_2 V_3 \cos(\theta_3 - \theta_2) + (Y_{13} + Y_{23}) V_3^2. \quad (26)$$

A. Small-Signal Model

Define $\theta_1' := \theta_1 - \delta$, $\theta_2' := \theta_2 - \delta$, $\theta_3' := \theta_3 - \delta$, $\theta_{13}' := \theta_1' - \theta_3'$, $\theta_{23}' := \theta_2' - \theta_3'$. Then, the small-signal model that results from linearizing (19) – (26) is given by

$$\frac{d}{dt}\begin{bmatrix} \Delta\omega \\ \Delta T_m \end{bmatrix} = A_m \begin{bmatrix} \Delta\omega \\ \Delta T_m \end{bmatrix} + B_m \begin{bmatrix} \Delta V_1 \\ \Delta \theta_1' \end{bmatrix}, (27)$$

where

$$A_m = \begin{bmatrix} -\frac{D}{M} & \frac{1}{M} \\ -\frac{1}{T_{SV} R_D \omega_s} & -\frac{1}{T_{SV}} \end{bmatrix},$$

$$B_m = \begin{bmatrix} 0 & 0 \\ \frac{E}{MX_m}\sin\theta_{1o}' & \frac{EV_{1o}}{MX_m}\cos\theta_{1o}' \\ 0 & 0 \end{bmatrix}, \quad (28)$$

and

$$\begin{bmatrix} \Delta P_w \\ \Delta Q_w \\ 0 \\ 0 \\ 0 \\ 0 \end{bmatrix} = \begin{bmatrix} 0 & C_{12} \\ C_{21} & C_{22} \end{bmatrix} \begin{bmatrix} \Delta V_1 \\ \Delta \theta_1' \\ \Delta V_2 \\ \Delta V_3 \\ \Delta \theta_{13}' \\ \Delta \theta_{23}' \end{bmatrix}, \quad (29)$$

where C_{12}, C_{21}, and C_{22} are defined in (18), and where ΔP_w is given by

$$\Delta P_w \in \Omega_{\Delta P_w} = \{\Delta P_w : |\Delta P_w| \leq k_w P_m\},$$
$$\Delta Q_w = 0, \quad (30)$$

Then, following the notation of (7), the small-signal model can be rewritten as

$$\frac{d}{dt}\begin{bmatrix} \Delta\omega \\ \Delta T_m \end{bmatrix} = A \begin{bmatrix} \Delta\omega \\ \Delta T_m \end{bmatrix} + B \begin{bmatrix} \Delta P_w \\ \Delta Q_w \end{bmatrix}, \quad (31)$$

where $A = A_m$, and $B = -B_m(C_{12}C_{22}^{-1}C_{21})^{-1}$.

B. Reachability Numerical Analysis

Reachability analysis of system (31) was conducted using the parameter values in Table II where all values are given in per unit unless otherwise specified. The nominal value of the wind-based power generation, $P_m = 0.4$ p.u. represents 40% of the total demand at bus 2. A steady-state power flow study was conducted to obtain all the equilibrium voltage magnitudes and angles needed in the linearized model, which yielded the following results: $E_{1o} = 1.13$ p.u., $V_{1o} = 1$ p.u., $V_{2o} = 0.94$ p.u., $V_{3o} = 0.94$ p.u., $\theta_{1o}' = -6.12°$, $\theta_{13o}' = 3.65°$, $\theta_{23o}' = 3.89°$. The reach set for the linearized system (31), which is depicted in Fig. 4, is the result of 30% variation in P_w around the nominal value. It can be seen that the reach set is entirely contained within the region defined by the solid vertical traces,

$$C_{12} = \begin{bmatrix} Y_{23} V_{3o} \sin\theta_{23o}' & Y_{23} V_{2o} \sin\theta_{23o}' & 0 & Y_{23} V_{2o} V_{3o} \cos\theta_{23o}' \\ -Y_{23} V_{3o}\cos\theta_{23o}' + 2Y_{23} V_{2o} & -Y_{23} V_{2o}\cos\theta_{23o}' & 0 & Y_{23} V_{2o} V_{3o}\sin\theta_{23o}' \end{bmatrix},$$

$$C_{21} = \begin{bmatrix} Y_m E \sin\theta_{1o}' + Y_{13} V_{3o}\sin\theta_{13o}' & Y_m E V_{1o}\cos\theta_{1o}' \\ Y_m E\cos\theta_{1o}' + Y_{13} V_{3o}\cos\theta_{13o}' - 2(Y_{13} + 2Y_m)V_{1o} & -Y_m E V_{1o}\sin\theta_{1o}' \\ Y_{13} V_{3o}\sin\theta_{13o}' & 0 \\ Y_{13} V_{3o}\cos\theta_{13o}' & 0 \end{bmatrix},$$

$$C_{22} = \begin{bmatrix} 0 & Y_{13} V_{1o}\sin\theta_{13o}' & Y_{13} V_{1o} V_{3o}\cos\theta_{13o}' & 0 \\ 0 & Y_{13} V_{1o}\cos\theta_{13o}' & -Y_{13} V_{1o} V_{3o}\sin\theta_{13o}' & 0 \\ Y_{23} V_{3o}\sin\theta_{23o}' & Y_{13} V_{1o}\sin\theta_{13o}' + Y_{23} V_{2o}\sin\theta_{23o}' & Y_{13} V_{1o} V_{3o}\cos\theta_{13o}' & Y_{23} V_{2o} V_{3o}\cos\theta_{23o} \\ Y_{23} V_{3o}\cos\theta_{23o}' & Y_{13} V_{1o}\cos\theta_{13o}' + Y_{23} V_{2o}\cos\theta_{23o}' - 2(Y_{13} + Y_{23})V_{3o} & -Y_{13} V_{1o} V_{3o}\sin\theta_{13o}' & -Y_{23} V_{2o} V_{3o}\sin\theta_{23o} \end{bmatrix} \quad (18)$$

which, as before, represent the acceptable frequency range of the WECC system. However, these results may be optimistic due to the simplified machine model used. A complete turbine-generator model should be used in order to verify whether or not the system can respond to such large variations in the wind-based power generation.

V. CONCLUDING REMARKS

This paper proposes a method for assessing the impact of uncontrolled disturbances on power system dynamic performance. In particular, we focus on the impact of uncontrolled wind power fluctuations. This method is useful to determine whether or not certain system variables may deviate from prescribed values imposed by operational requirements. We provide an analytically tractable method based on reachability analysis techniques for dynamical systems, that allows us to approximate the system reach set by the reach set of the linearized system model around some nominal value.

Further work will include a formal analysis of the limits of small-signal reachability analysis for power systems, i.e., how large can the deviations on the uncontrolled disturbance be so that the approximation of the true reach set by the reach set of the linearized model is valid. Another aspect to be investigated is whether or not the small-signal reach set upper bounds the exact reach set or on the contrary, it is not possible to make any general statements on this matter. The SMIB results suggest that, for this case, the linearized model reach set is an upper bound on the system exact reach set. The scalability of the proposed method also needs to be

further investigated. More accurate models of the wind-based power injections will also be proposed. In this regard, wind-based power injections, instead of assuming they are an unknown-but-bounded quantity, they could be governed by a differential equation with a driving force representing wind speed that is unknown-but-bounded itself. Thus, instead of bounding the wind-based power injection forecast error, a bound would be placed on the wind speed forecast error. This would us to also allow include limits on the time derivatives on wind-based power injections.

REFERENCES

[1] E. Hirst, "Integrating wind output with bulk power operations and wholesale electricity markets," *Wind Energy*, vol. 5, no. 1, pp. 19–36, 2002.

[2] P. Eriksen, T. Ackermann, H. Abildgaard, P. Smith, W. Winter, and J. R. Garcia, "System operation with high wind penetration," *IEEE Power and Energy Magazine*, vol. 3, no. 6, pp. 65–74, Nov.-Dec. 2005.

[3] E. DeMeo, G. Jordan, C. Kalich, J. King, M. Milligan, C. Murley, B. Oakleaf, and M. Schuerger, "Accommodating wind's natural behavior," *IEEE Power and Energy Magazine*, vol. 5, no. 6, pp. 59–67, Nov.-Dec. 2007.

[4] M. Ahlstrom, L. Jones, R. Zavadil, and W. Grant, "The future of wind forecasting and utility operations," *IEEE Power and Energy Magazine*, vol. 3, no. 6, pp. 57–64, Nov.-Dec. 2005.

[5] "Planning of the grid integration of wind energy in germany onshore and offshore up to the year 2020," Deutsche Energie-Agentur GmbH, Berlin, Ge, Tech. Rep., February 2005.

[6] D. Gautam, V. Vittal, and T. Harbour, "Impact of increased penetration of dfig-based wind turbine generators on transient and small signal stability of power systems," *IEEE Transactions on Power Systems*, vol. 24, no. 3, pp. 1426–1434, Aug. 2009.

[7] T. Ackermann, G. Ancell, L. Borup, P. Eriksen, B. Ernst, F. Groome, M. Lange, C. Mohrlen, A. Orths, J. O'Sullivan, and M. de la Torre, "Where the wind blows," *IEEE Power and Energy Magazine*, vol. 7, no. 6, pp. 65–75, November-December 2009.

[8] P. Sauer and A. Pai, *Power System Dynamics and Stability*. Upper Saddle River, NJ: Prentice Hall, 1998.

[9] F. Schweppe, *Uncertain Dynamic Systems*. Englewood Cliffs, NJ: Prentice-Hall Inc., 1973.

[10] F. Alvarado, Y. Hu, and R. Adapa, "Uncertainty in power system modeling and computation," in *Proc of the IEEE International Conference on Systems, Man and Cybernetics*, Oct 1992.

[11] Z. Wang and F. Alvarado, "Interval arithmetic in power flow analysis," *IEEE Transactions on Power Systems*, vol. 7, no. 3, pp. 1341–1349, Aug 1992.

[12] A. Saric and A. Stankovic, "Applications of ellipsoidal approximations to polyhedral sets in power system optimization," *IEEE Transactions on Power Systems*, vol. 23, no. 3, pp. 956–965, Aug. 2008.
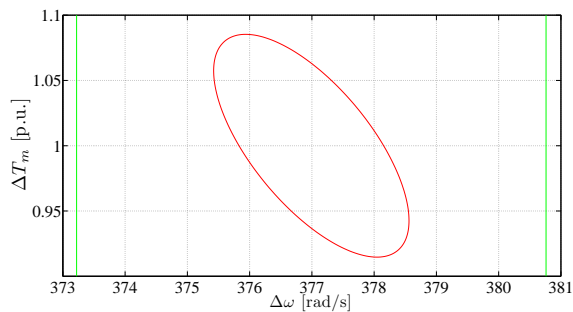
Fig. 4. Wind power injection model reachability analysis results.

[13] J. L. Jin, H. Liu, R. Kumar, V. Ajjarapu, J. McCalley, N. Elia, and V. Vittal, "An application of reachable set analysis in power system transient stability assessment," in *Proc. of the IEEE Power Engineering Society General Meeting*, June 2005.

[14] I. Hiskens and M. Pai, "Trajectory sensitivity analysis of hybrid systems," *IEEE Transactions on Circuits and Systems I: Fundamental Theory and Applications*, vol. 47, no. 2, pp. 204 –220, feb 2000.

[15] I. Hiskens and J. Alseddiqui, "Sensitivity, approximation, and uncertainty in power system dynamic simulation," *IEEE Transactions on Power Systems*, vol. 21, no. 4, pp. 1808 –1820, nov. 2006.

[16] D. Angeli and E. Sontag, "Forward completeness, unboundedness observability, and their lyapunov characterizations," *Systems Control Letters*, vol. 38, no. 4-5, pp. 209–217, 1999.

[17] E. Sontag, "Smooth stabilization implies coprime factorization," *IEEE Transactions on Automatic Control*, vol. 34, no. 4, pp. 435–443, Apr 1989.

[18] M. Müller and A. Domínguez-García, "On input-to-state stability notions for reachability analysis of power systems," in *Proc. of the IEEE International Symposium on Circuits and Systems*, Paris, France, 2010.

[19] M. Athans and P. Falb, *Optimal Control: An Introduction to the Theory and its Applications*. New York, NY,: McGraw-Hill, 1966.

[20] A. Kurzhanski and P. Varaiya, "Ellipsoidal techniques for reachability analysis. parts I & II," *Optimization Methods and Software*, vol. 17, pp. 177–206 and 207–237, February 2002.

[21] Western Electricity Coordinating Council (WECC). WECC coordinated off-nominal frequency load shedding and restoration requirements. [Online]. Available: http://www.wecc.biz/library/default.aspx